CrossMark

Heavy precipitation in the southwest of Iran: association with the Madden–Julian Oscillation and synoptic scale analysis

M. Jafar Nazemosadat[1] · K. Shahgholian[1]

Abstract Some important characteristics of the November–April heavy precipitation in southwestern parts of Iran and their linkages to the Madden–Julian Oscillation (MJO) were assessed for the period of 1975–2011. Daily precipitation data in nine meteorological stations spread in various parts of the study area and the corresponding MJO indices were analyzed. For each station, precipitation data were sorted in descending order and those values that fell within 5% of the highest records were categorized as the heavy precipitation. Besides this, the 10% threshold was also analyzed as an axillary assessment. The considered heavy precipitation data (5% threshold) accounted from about 26–35% of total annual precipitation. About half of the heavy precipitation occurred during December–January period and the other half distributed within the months of March, February, November and April by about 17, 14, 13and 6%, respectively. The highest frequency of heavy precipitation was related to the MJO phase 8. After this, the more frequent precipitation events were respectively associated to the phases 2, 7, 1, 6, 5 and 4 of the MJO. For the phases 1, 2, 7 and 8 frequency of the heavy precipitation statistically increased when the MJO amplitude was greater than unity. In contrast, for phases 4 and 5, heavy precipitation was generally linked to the spells that the amplitude size was lower than unity. Formation of a strong north–south oriented cold front mainly in Saudi Arabia and west-east oriented warm fronts in the southwest of Iran were realized as the key elements for initiating heavy precipitation over the study area. Although development of the Mediterranean-based cyclonic circulation is essential for the formation of these fronts, moisture transport mostly originates from northern parts of the Arabian Sea, southern parts of the Red Sea and the Persian Gulf.

1 Introduction

Because of the rapid growth of world population and recent improvement in the living standards, water demand for agriculture, sanitation, drinking, manufacturing and leisure are ever-increasing worldwide. Since precipitation is a vital component of climate system, understanding the mechanism of precipitation production is essential for comprehensive management of climatic hazards and the restricted freshwater resources. Analyzing the impacts of large scale tele-connection patterns such as the El Niño-Southern Oscillation (ENSO) and the Madden Julian Oscillation (MJO) on precipitation variability have been widely used as a tool for the prediction of precipitation characteristics and its subsequent water management.

Recent studies have shown that ENSO in conjunction with variations in the sea surface temperatures (SSTs) over tropical and extra-tropical water bodies induce a significant impact on precipitation variability and climate change in Iran and West Asia (Nazemosadat and Cordery 2000; Nazemosadat 2001; Nazemosadat and Ghasemi 2004; Nazemosadat et al. 2006; Barlow et al. 2002; Hoell et al. 2013a, b, 2014; Hoell and Funk 2013). These studies

✉ K. Shahgholian
nadiashahgholian@gmail.com

M. Jafar Nazemosadat
jafar@shirazu.ac.ir

[1] Water Engineering Department, College of Agriculture, Atmospheric and Oceanic Research Center (AORC), Shiraz University, Shiraz, Iran

infer that, for Iran and most of the Middle Eastern countries, above or below normal precipitation are generally associated to the warm or cold ENSO events, respectively. Furthermore, compare to other months of the year, this association is more significant for the October–December period. Nazemosadat and Ghasemi (2004) showed that, during La Nina events, the combination of the ENSO indices with the Bengal Gulf SSTs is an efficient approach for the prediction of dryness or wetness in Iran during boreal winter. Nazemosadat et al. (2006) have shown that the change-point years in the Iran's precipitation time-series are significantly coherent with the change-point years in the SOI time-series.

In addition to ENSO, a number of investigators demonstrated that variation in the MJO cycle also induces a clear influence on the precipitation variability and atmospheric circulation in various parts of the world. According to these studies, besides tropical climate, MJO also affects extra-tropical weather and climate systems (Barlow et al. 2005; Bond and Vecchi 2003; Carvalho et al. 2004; Donald et al. 2006; Ferranti et al. 1990; Jones 2000; Hung et al. 2014; Liebmann and; Hartmann 1984; Krishnamurti et al. 1997). The MJO also strongly influences the monsoonal precipitation in Asia and Australia, and moderately affects precipitation variability in North and South America (Lau and Chan 1986; Mo 2000; Nogués-Paegle et al. 2000; Higgins and Shi 2001; Carvalho et al. 2004; Donald et al. 2006; Hoell et al. 2012). Donald et al. (2006) have provided a mechanistic basis for an MJO-based intra-seasonal forecasting capacity that bridges the weather-climate divide.

It has been shown that MJO significantly influences climate variability in Southwest Asia including most parts of Iran (Barlow et al. 2005, 2002; Nazemosadat and Ghaedamini 2010; Hoell et al. 2012, 2015; Hoell and Funk 2013). Nazemosadat and Ghaedamini (2010) categorized combination of the phases 1, 2, 7 and 8 of the MJO as the negative and phases 3, 4, 5 and 6 as the MJO positive phase. They showed that prevalence of the positive or negative MJO phase suppresses or enhances precipitation over the Arabian Peninsula and southern parts of Iran, respectively. Pourasghar et al. (2015) have analyzed the MJO-precipitation relationships in Iran using precipitation data collected over 183 stations mostly located in southern parts of the country. Their findings generally support the concluded remarks by Nazemosadat and Ghaedamini (2010) about Iran. They reported wet conditions in southern parts of Iran during the MJO phases 1–2 and 7–8. During these phases, atmospheric circulation anomalies favor moisture advection from western parts of the Indian Ocean into southern Iran. In contrast, dry conditions during MJO phases 3–6 are associated with advection of drier air from the north. Despite these valuable works, it is fair to say that the MJO and its effects on climate variability remains an

unmet challenge to our understanding of the tropical and extra-tropical atmospheres (Zhang 2005; Liu et al. 2016; Zaitchik 2017).

The MJO cycle presented here is an accepted standard definition introduced by Wheeler and Hendon (2004) [hereafter WH 2004]. Based on this definition the MJO cycle is split up into 8 phases so that each phase corresponds to 1/8 of the full cycle. An individual MJO event generally lasts between 30 and 60 days. For better demonstration of the contributions of both convective activities and dynamical features of the Oscillation, a number of investigators utilized various approaches to improve the quality of the WH 2004 index (Ventrice et al. 2013; Kiladis et al. 2014; Liu 2014; Adames and Wallace 2014, 2015; Liu et al. 2016). In spite of these qualified investigations, our preliminary examination indicated that the observational precipitation data is more compatible with the utilized gridded data if the application of WH 2004 rather than the velocity potential MJO (VPM as indicated in Ventrice et al. 2013) was used as the MJO index.

Masudian and Jafari Shendi (2015) analyzed heavy precipitation over some areas of Iran categorized as the 'northern low rainfall region'. They concluded that development of a high pressure system over the Siberia-Black Sea region and formation of a low pressure system over the Red Sea-Persian Gulf areas are the main causes of these precipitation events. According to Masoodian and Mohammadi (2012) heavy precipitation in Iran is mostly due to the moisture transport through the near surface pressure levels. The Caspian Sea, Persian Gulf and Arabian Sea were realized as the main sources of the studied heavy precipitation in Iran (Masoudian 2009). Alijani et al. (2007) reported that coastal areas in southern parts of Iran and the foothills of Zagros Range in southwestern districts of the country are seriously exposed to the risk of extreme rainfall and heavy precipitation. Alijani et al. (2010) characterized heavy precipitation in southeastern parts of Iran as: (1) a strong moisture discharge from the Persian Gulf at the low atmospheric levels (2) positioning the subtropical jet stream in the western edge of the precipitating area and (3) strong negative anomalies of the omega data in the mid troposphere.

The aforementioned references about heavy precipitation in Iran suggested that the characteristics of this precipitation do not follow an identical pattern in various parts of the country and further works are needed to understand the mechanism of this precipitation. These studies generally performed Factor Analysis to categorize a few specific precipitating days as the spells with heavy precipitation. Main aspects of atmospheric circulation were then analyzed for these limited daily events. In spite of these valuable efforts, the method of detecting heavy precipitation, compositing precipitation data with other atmospheric variables and tracking weather systems for a few successive days as
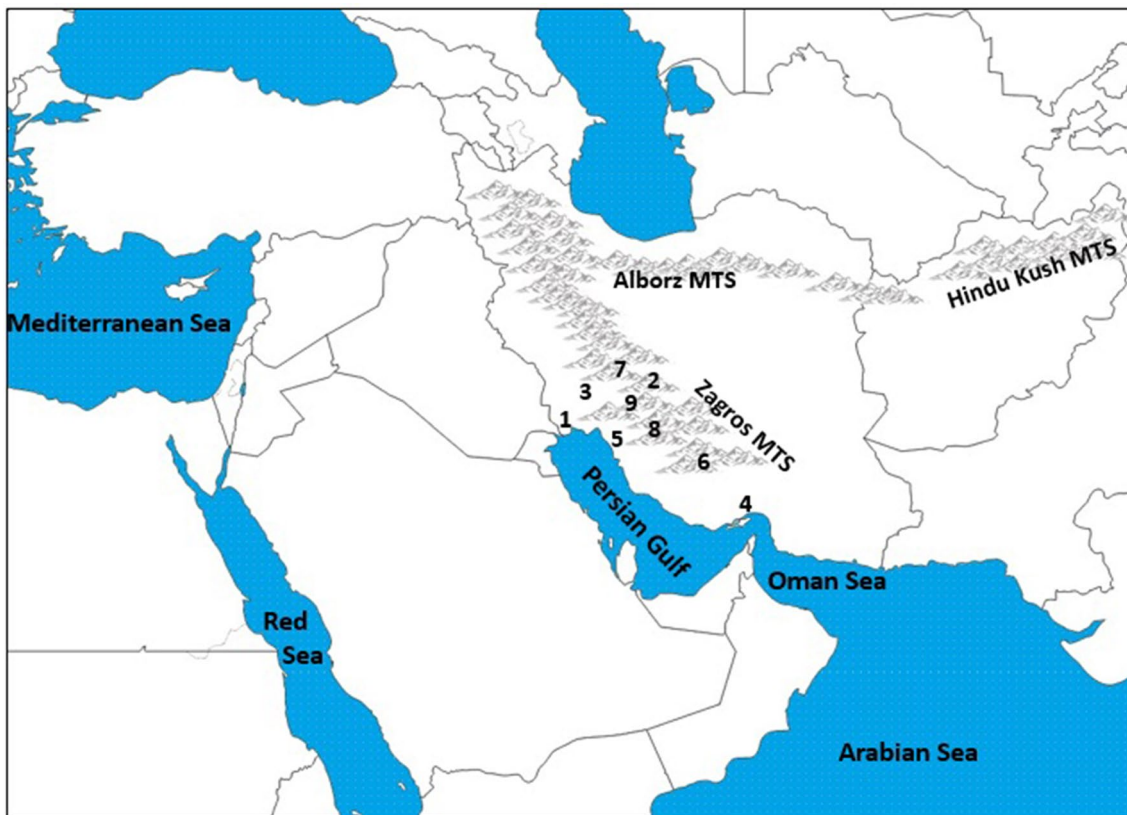
Fig. 1 Geographical location of the studied stations in southwestern parts of Iran. Approximate situation of the Alborz and Zagros ranges that are oriented in the northwest-northeast and northwest–southeast directions are presented, respectively. The selected stations are generally positioned within the Zagros Ranges. The presented numbers inside the map refer to the position of the rain-gauge stations whose names are indicated in column 2 of Table 1

conducted in this study were not the themes of the previous studies. More importantly, investigating possible linkage between heavy precipitation in Iran and various phases of the MJO were not studied in the previous works. It is noteworthy to mention that, compare to other parts of Iran, precipitation variability in southwestern districts is more sensitive to the alternation in the MJO phases (Nazemosadat and Ghaedamini 2010; Nazemosadat and Shahgolian 2014; Pourasghar et al. 2015). Due to such sensitivity, the present study motivated to analyze the associations between MJO phases and heavy precipitation for this part of the country.

We utilized our own methodology to specify heavy precipitation in southwestern parts of Iran during the November–April period. After examining some statistical properties of the detected heavy precipitation, frequency analysis was performed to clarify monthly distribution of this precipitation. The study then examined the frequency of heavy precipitation during various phases of the MJO. The effect of the MJO amplitude size on the frequency, intensity and total precipitation were then investigated. Images related to the spatial distribution of mean heavy precipitation and some other atmospheric variables were produced from a day before to a day after heavy precipitation to explore the spatio-temporal features of the pervasive precipitation events. Mechanism of the formation of weather fronts and moisture transport to the study area were finally discussed.

2 Data

2.1 MJO index

Daily values of the MJO amplitude and its associated phase numbers were extracted from the website of the Australian Bureau of Meteorology Research Centre for the period of 1975–2011 in daily timescale (Wheeler and Hendon 2004). These data were then composited with the station-based records of heavy precipitation in each individual station.

2.2 Precipitation

The November–April daily precipitation data of nine synoptic stations spread in various parts of southwestern Iran were obtained for the period 1975–2011 (36 years). These data were gratefully extracted from the websites of either Iranian Meteorological Organization (IRIMO)

Table 1 The name, elevation and some statistical properties of the utilized precipitation data

Station no.	Station name	Elevation (m)	Record length (year)	Frequency of pre-cipitating days	Percentage of days[a]	Total precipitation (mm)	Mean precipitation (mm/day)[b]
1	Abadan	6.6	36	1060	7.8	5715	5.4
2	Abadeh	2030	34	1291	10.1	4773	3.7
3	Ahwaz	22.5	36	1309	9.6	8122	6.2
4	Bandar-Abbas	9.8	36	702	5.2	6540	9.3
5	Bushehr	19.6	36	1218	9.0	8987	7.4
6	Lar	792	19	476	6.5	3728	7.8
7	Shahrekord	2049	36	1738	12.8	11,481	6.6
8	Shiraz	1484	36	1475	10.9	11,538	7.8
9	Yasuj	1831.5	21	1231	17.0	18,151	14.8

Numbers inside Fig. 1 represent the station names as indicated in column 2

[a]The precentage is obtained by dividing the frequency of precipitating days to the total days of the November–April period for 36 years

[b]Total precipitation is divided by total number of precipitating days

or the Koninklijk Nederlands Meteorologisch Instituut (KNMI). Geographical location of the selected stations and some statistical properties of the utilized precipitation time series are shown in Fig. 1 and Table 1, respectively. For instance, as indicated in Table 1, for Shahrekord station, out of 13,514 days of the study period (six months of a year), weather was in precipitating condition for only 1738 days or 12.8% of the period. The mean and total precipitation values during these 1738 days were 6.6 mm/day and 11,481 mm, respectively. Furthermore, among these nine stations, the highest or lowest value of precipitation rate is 14.8 mm/day or 4.1 mm/day that was recorded in Yasuj or Abadeh, respectively (Table 1). Although daily precipitation data were also available for a few of other stations, their reliability was not confirmed for utilizing in the present study. Furthermore, the applied data were found to be reasonable for the presented discussion. Missed data which were estimated to be around 1.5% of the total records, were excluded from further analysis and the obtained results are, therefore, based on the observational records.

2.3 Atmospheric variables

In addition to the observed ground-based precipitation data, gridded data of some atmospheric variables including precipitation rate, the 850 and 700-hPa wind vector (u and v components), air temperature and specific humidity were also utilized. These data were gratefully extracted from the website of the National Oceanic and Atmospheric Administration (NOAA). Images related to these variables were then produced in various spatiotemporal domains using the NOAA-ESRL compositing facilities.

3 Methodology

For each of the selected stations, daily precipitation data were firstly sorted in descending order and those values that fell within 5% of the highest records were categorized as heavy precipitation (Groisman et al. 2004). For assessing the possible effect of the selected threshold on the results, in addition to this 5%, the 10% threshold was also examined. Since significant inconsistency was not observed by changing the thresholds, the given discussions are mostly based on the 5% level although some relevant statistics are also presented for 10% threshold.

In the previous example for Shahrekord, after ranking daily precipitation data, 86 days with the highest value of daily precipitation (5%* 1720 = 86) were chosen as the heavy precipitation days. The dates of these records were spread throughout various cold months of the year and different phases of the MJO as will be discussed in the next sections. Among these 86 days, the magnitudes of the lightest, heaviest and mean precipitation were 24.0, 88.8 and 34.4 mm/day (Table 2), respectively. As indicated, while the lightest precipitation occurred in January and phase 3 of the MJO, the heaviest precipitation happened in December and phase 1. Table 2 specifies phase number and amplitude size of the MJO for the lightest and heaviest precipitation events in each of the studied sites. The dates and some other characteristics of these 86 precipitation events were then used for constructing the MJO-precipitation composites. These composites were obtained for each month of the November–April period and for each of the MJO phase.

By using the NOAA-ERSL compositing facilities, besides the station-based precipitation data, similar composites were also constructed for all of the utilized

Table 2 Some statistical features of the detected heavy precipitation events (upper 5% level)

Stations no	Stations name	Frequency of heavy precipitation days	Lightest intensity (mm/day)	Heaviest intensity (mm /day)	Total heavy precipitation (mm)	Mean of heavy precipitation (mm/day)
1	Abadan	53	21.2 (1,3)*	86.0 (6,4)*	1790.8 (31.3%)* *	34.0
2	Abadeh	52	15.1 (7,3)	83.0 (2,12)	1511.0 (35.8%)	29.1
3	Ahwaz	65	24.3 (1,11)*	107.0 (1,11)*	2428.1 (29.9%)* *	37.1
4	Bandar-Abbas	35	39.0 (8,1)*	211.0 (1,1)*	2177.0 (33.3%)* *	57.8
5	Bushehr	61	33.2 (5,1)*	144.0 (1,1)*	3060.7 (34.1%)* *	48.6
6	Lar	24	30.0 (2,3)	102.0 (7,2)	1185.2 (31.8%)	49.4
7	Shahrekord	86	24.0 (3,1)*	88.8 (1,11)*	2954.9 (25.7%)* *	34.4
8	Shiraz	74	29.0 (1,1)*	99.0 (1,12)*	3117.9 (27.0%)* *	42.0
9	Yasuj	62	57.0 (2,11)*	135.0 (8,1)*	4761.4 (26.2%)* *	76.7

*In columns 4 and 5, numbers inside the parentheses denote the MJO phase number and month of the year, respectively. While month 1 denotes January, 12 signifies December

**In column 6, numbers inside the parentheses show the ratio of total heavy precipitation to total long-term precipitation in percentage

Table 3 Like Table 2 except for 10% threshold

Row	Stations	Frequency of heavy precipitation days	Lightest (mm/day)	Heaviest (mm /day)	Total heavy precipitation (mm) (%)	Mean of heavy precipitation (mm/day)
1	Abadan	105	14.4 (5,1)*	86.0(6,4)*	2707.3 (47.4)**	25.8
2	Abadeh	104	11.5 (2,1)	83.0 (2,12)	2193.2 (52.0)	21.1
3	Ahwaz	130	17.3 (8,3)*	107.0 (1,11)*	3719.6 (45.8)**	24.8
4	Bandar-Abbas	70	25.0 (6,1)*	211.0 (1,1)*	3297.1 (50.4)**	44.7
5	Bushehr	122	21.0 (8,12)*	144.0 (1,1)*	4642.2 (51.6)**	37.1
6	Lar	48	21.0 (8,4)*	102.0 (7,2)	1766.7 (47.4)	36.8
7	Shahrekord	172	17.6 (4,2)*	88.8 (1,11)*	4694.6 (40.9)**	27.3
8	Shiraz	146	21.7 (1,2)*	99.0 (1,2)*	4917.2 (42.6)**	33.6
9	Yasuj	123	38.4 (3,11)*	135.0 (8,1)*	7582.0 (41.8)**	61.4

*In columns 4 and 5, numbers inside the parentheses denote the MJO phase number and month of the year, respectively. While month 1 denotes January, 12 signifies December

**In column 6, numbers inside the parentheses show the ratio of total heavy precipitation to total long-term precipitation in percentage

atmospheric gridded data. Although the presented synoptic scale analyses are mostly focused on 74 days of heavy precipitation at Shiraz station (Table 1; Fig. 1), Appendix contains some important illustrations for the other stations. These illustrations confirm that the presented synoptic weather analysis covers the main characteristics of heavy precipitation over the study area.

The Grads software was used for manipulating and overlaying the desired images. This software was also used for generating the vapor flux images that were produced by multiplication of vector winds and specific humidity as described in NOAA webpage[1].

4 Results and discussion

4.1 Some statistical features

Tables 2 and 3 delineate some statistical properties of heavy precipitation for the 5 and 10% thresholds. Consistency between the presented statistics of these two Tables suggests that the given result and discussions are not significantly influenced by the selected thresholds. As indicated in both Tables, in six stations including Ahwaz, Bandar-Abbas, Bushehr, Shahrekord, Shiraz and Yasuj, the heaviest precipitation has occurred in either phase 1 or phase 8 of the MJO. While the heaviest precipitation in Abadeh or Lar, respectively, happened in phase 2 or 7, Abadan precipitation exhibited a large coherence with phase 6.

Although, frequency of the heavy precipitation is comparatively small (maximum 86 days in Shahrekord for 36

---

[1] http://www.esrl.noaa.gov/psd/data/composites/day/calculation.html.

Table 4 Monthly distribution of heavy precipitation for 5% threshold

Row	Stations	Number of days	January	February	March	April	November	December	Total
1	Abadan	53	18.8	7.6	9.4	7.6	24.5	32.1*	100
2	Abadeh	52	17.3	9.6	25.0	9.6	5.8	32.7	100
3	Ahwaz	65	24.6	6.2	10.8	3.1	21.5	33.8*	100
4	Bandar-Abbas	35	17.1	37.1*	28.6	2.9	0.0	14.3	100
5	Bushehr	61	34.4*	6.6	11.5	0.0	13.1	34.4*	100
6	Lar	24	16.7	20.8	20.8	0.0	0.0	41.7	100
7	Shahrekord	86	19.7	13.9	22.1	4.8	15.1	24.4*	100
8	Shiraz	74	37.8*	13.5	9.5	1.3	6.8	31.1	100
9	Yasuj	62	22.5	19.4	20.9	4.8	6.6	25.8*	100
10	Mean values	62.3	23.2	15.0	17.6	3.8	10.4	30.0	100

In each row, the maximum value is flagged by *

Table 5 Like Table 4 except for 10% threshold

Row	Stations	Number of days	January	February	March	April	November	December	Total
1	Abadan	105	29.5*	7.6	14.3	7.6	15.2	25.8	100
2	Abadeh	104	15.4	12.5	25.0	10.6	8.6	27.9	100
3	Ahwaz	130	23.9	10.0	13.8	2.3	16.2	33.8*	100
4	Bandar-Abbas	70	27.1*	27.1*	22.9	2.9	2.9	17.1	100
5	Bushehr	122	32.8	10.7	7.4	0.0	14.7	34.4*	100
6	Lar	48	27.1	20.8	16.7	2.1	0.0	33.3	100
7	Shahrekord	172	20.4	15.7	19.2	9.8	11.6	23.3*	100
8	Shiraz	146	34.3*	14.3	14.4	4.1	8.2	24.7	100
9	Yasuj	123	22.0	18.7	21.1	4.8	8.1	25.3*	100
10	Mean values	124	25.8	15.3	17.2	4.9	9.5	27.3	100

In each row, the maximum value is flagged by *

years), this precipitation comprises from 25.7 to 35.8% of annual precipitation as is depicted in Table 2 (values in parenthesis flagged by **). These statistics deviate from 40.9 to 52.0% in Table 3. The given information suggests that, for the 5 or 10% threshold, heavy precipitation constitutes about 30 or 45% of total annual precipitation, respectively.

The most intense precipitation event with the rate of 211 mm/ day occurred on January 24, 1979 in Bandar-Abbas which was the continuation of a few rainy days in the southwest of Iran (Table 2). For this day, the phase number and amplitude size of the MJO were 1 and 2.1, respectively. It is noteworthy to mention that, from the second to 27th of January 1979, the Oscillation signals were mainly concentrated over the areas associated to the phases 7, 8 and 1. For this period, the MJO amplitudes were consistently strong and greater than unity. For the date of heavy precipitation in Bandar-Abbas the oceanic core center of precipitation was extended over the Indian Ocean equator, between 60° and 90° E. After this, the 144 mm/day rainfall in Bushehr on January 11, 2002 ranked as the second most intense precipitation. The phase and amplitude of MJO for this day were 1 and

1.0, respectively. For this day, precipitation events were mostly concentrated over tropical parts of the southern hemisphere between 60° and 80° E and between 160 and 180° E.

The two smallest values of the heavy precipitation data are associated to Abadeh and Abadan (respectively 83 mm/day and 86 mm/day in Table 2). Total heavy precipitation is also the lowest for these two stations indicating the inherent dryness condition of these areas. Although the elevation of Abadeh (2030 m) is higher than most of the considered stations, the city is located in a flat plain, far from the main passage of the incoming air-mass.

In spite of the fact that Shahrekord has the highest frequency of rainy days, mean daily precipitation of this station is almost the least, indicating less probability of hazardous flash flood for this station as compared with the areas such as Bandar-Abbas or Bushehr (Table 2). According to the given statistics in Table 2, during rainy seasons of the year, the probability for having precipitating day or heavy precipitating day in Shahrekord is only 12.8 or 0.636%, respectively. These two statistics that even drop to 5.2 and 0.26% for Bandar-Abbas, emphasize the severity of dryness over the study area.

Table 6 Frequency of heavy precipitation in each of the MJO phases in %

Row	Stations	Total frequency	1	2	3	4	5	6	7	8	Total
1	Abadan	53	15.1	5.7	11.4	9.4	5.7	11.2	<u>20.8</u>	<u>20.8</u>	100
2	Abadeh	52	9.8	15.7	9.8	13.7	5.9	7.8	<u>19.6</u>	17.7	100
3	Ahwaz	65	13.9	21.5	3.1	6.2	3.1	12.3	15.4	<u>24.6</u>	100
4	Bandar-Abbas	35	14.3	5.7	5.7	5.7	17.1	8.6	20.0	<u>22.9</u>	100
5	Bushehr	61	13.1	<u>24.6</u>	4.9	6.6	8.2	4.9	14.8	23.0	100
6	Lar	24	12.5	16.7	8.3	0.1	4.2	4.2	<u>37.5</u>	16.6	100
7	Shahrekord	86	16.3	15.1	11.6	7.0	5.8	14.0	8.1	<u>22.1</u>	100
8	Shiraz	74	12.2	18.9	2.7	8.1	4.1	20.3	12.2	<u>21.6</u>	100
9	Yasuj	62	12.9	<u>25.8</u>	8.1	0.0	6.5	17.7	12.9	16.1	100
10	Mean values	62.3	13.3	16.6	7.3	6.3	6.7	11.2	17.9	<u>20.6</u>	100

Numbers 1 to 8 delineate phase number of the MJO

The maximum values are underlined

Table 7 Like Table 6 except for 10% threshold

Row	Stations	Number of days	1	2	3	4	5	6	7	8	Total
1	Abadan	105	10.5	13.3	8.6	6.7	7.6	16.2	17.1	<u>20.0</u>	100
2	Abadeh	104	11.7	<u>18.5</u>	12.6	11.7	3.9	7.8	17.5	16.5	100
3	Ahwaz	130	14.6	13.1	6.9	3.1	10.0	15.4	11.5	<u>25.4</u>	100
4	Bandar-Abbas	70	12.9	4.3	10.0	7.1	14.3	12.9	14.3	<u>24.3</u>	100
5	Bushehr	122	9.0	<u>26.2</u>	7.4	4.9	8.2	12.3	13.1	18.9	100
6	Lar	48	12.5	20.8	6.3	2.1	8.3	8.3	<u>22.9</u>	18.8	100
7	Shahrekord	172	15.1	14.5	12.2	5.8	7.0	12.2	14.0	<u>19.2</u>	100
8	Shiraz	146	13.7	15.8	8.2	6.2	8.2	15.1	15.8	<u>17.1</u>	100
9	Yasuj	123	12.2	<u>23.6</u>	8.1	5.7	7.3	12.2	13.8	17.1	100
10	Mean values	124	12.5	16.7	8.9	5.9	8.3	12.5	15.6	19.7	100

5 Monthly distribution

Tables 4 and 5 depict monthly distribution of heavy precipitation for the 5 and 10% thresholds, respectively. Among the presented statistics in these Tables, frequency of the precipitating days is strongly related to the record lengths of the applied data. The other statistics, however, are less associated to the study period and could, therefore, be considered as the long-term behavior of the precipitation. For example, in Table 4, out of 702 precipitating days in Bandar-Abbas, 35 daily events with mean of 57.8 mm/day (Table 2) were assigned as heavy precipitation. Out of these 35 days, for 13 or 10 days (37.14 or 28.6%), precipitation occurred in February or March, respectively. According to Table 4, December–January period is the most probable months for the occurrence of heavy precipitation in southwestern parts of Iran. After these two months, heavy precipitation concentrates on March and February, respectively. Almost similar ranking is also evident for the 10% threshold in Table 5. In overall, about 53.2% of total heavy precipitation is associated to the December–January period (30 + 23.2% = 53.2%). This statistic escalates to about 70.8, 85.8 and 96.2%, when the precipitating days during the

months of March, February and November are included, respectively (last row in Table 4). For Shahrekord, monthly distribution of heavy precipitation is more uniform than the other stations and inconsistency is less between various months.

Contrary to other stations, the occurrence probability of heavy precipitation in Bandar-Abbas is greater during March as compared to the December–January period. This finding is consistent with the conclusion of Nazemosadat and Ghaedamini (2010) who reported that, compared to December–February, the passage of rain-bearing airflows in southern parts of Iran shift to the east during the March–April period.

5.1 Phase dependence

The phase-based distribution of heavy precipitation is shown in Table 6. As indicated, for Ahwaz, Bandar-Abbas, Shahrekord and Shiraz, a large portion of heavy precipitation has occurred in phase 8. In Abadan, phases 7 and 8, each one with 20.8%, have the greatest contribution. The largest part of heavy precipitation in Yasuj and Bushehr is associated to phase 2. Heavy precipitation in Lar is highly

Table 8 Frequency of heavy precipitation for the spells that the Oscillation amplitudes are greater or less than unity, (Amp > 1 or Amp < 1 respectively)

Row	Station	MJO phase	1	2	3	4	5	6	7	8	Total precipitating days	Total precipitation mm	Mean precipitation mm/day	Ratio of frequency
1	Abadan	Amp > 1	6	2	3	5	1	6	11	7	41	1407.3	34.3	3.4
		Amp < 1	2	1	3	0	2	0	0	4	12	446.5	37.2	
2	Abadeh	Amp > 1	3	6	3	5	1	3	8	5	34	1473	43.3	1.9
		Amp < 1	2	2	2	2	2	1	2	5	18	720.2	40.0	
3	Ahwaz	Amp > 1	6	9	0	3	0	4	9	9	40	1513.6	37.8	1.6
		Amp < 1	3	5	2	1	2	4	1	7	25	914.5	36.6	
4	Bandar-Abbas	Amp > 1	4	1	2	0	3	1	6	6	23	1470.2	63.9	1.9
		Amp < 1	1	1	0	2	3	2	1	2	12	706.8	58.9	
5	Bushehr	Amp > 1	5	11	2	1	3	0	9	9	40	2011.2	50.3	1.9
		Amp < 1	3	4	1	3	2	3	0	5	21	1049.5	50.0	
6	Lar	Amp > 1	2	4	1	0	0	1	9	2	19	906.7	47.7	3.8
		Amp < 1	1	0	1	0	1	0	0	2	5	278.5	55.7	
7	Shahrekord	Amp > 1	13	10	5	3	2	9	6	11	59	2237.6	37.9	2.2
		Amp < 1	1	3	5	3	3	3	1	8	27	995.2	36.9	
8	Shiraz	Amp > 1	5	10	1	3	0	9	7	9	44	1753.5	39.9	1.5
		Amp < 1	4	4	1	3	3	6	2	7	30	1364.4	45.5	
9	Yasuj	Amp > 1	5	11	4	0	2	8	8	7	45	3479.8	77.3	2.6
		Amp < 1	3	5	1	0	2	3	0	3	17	1281.6	75.4	
	Total	Amp > 1	49	64	21	20	12	41	73	65	345	16,253	432	2.3
		Amp < 1	20	25	16	14	20	22	7	43	167	7757	436	

In the first row, numbers 1 to 8 refer the MJO phase number

probable in phase 7. In overall, the occurrence probability of heavy precipitation in southwestern parts of Iran is highest for the MJO phases 8 as compared to the other phases. After this, the probability is respectively higher for the phases 2, 7, 1, 6, 5 and 4. With the exception of Lar and Yasuj, at least one incident of heavy precipitation occurred in each of the eight phases of MJO.

The lowest probability for having heavy precipitation is related to the spells that MJO signals are concentrated on either phase 5 or particularly phase 4. Consistency between the presented statistics in Tables 6 and 7 suggests the inconsiderable effects of the selected thresholds on the presented discussion.

5.2 Effects of the amplitude size

The influence of the MJO amplitude size on the intensity and frequency of heavy precipitation was examined by comparing these statistical properties between the spells that the amplitudes were either greater or less than unity. For instance, as indicated in Table 8, out of 74 heavy precipitation events at Shiraz station, 30 or 44 events were associated to the spells that the amplitudes were below or above unity, respectively. The mean daily precipitation

rate for these two sets of events was accordingly, 45.5 and 39.9 mm (column 14 in Table 8). As indicated, precipitation rates do not show significant difference between the spells that the amplitudes are below or greater than 1.0.

The ratio of precipitation frequency during the spells that the amplitude size was greater than unity to the corresponding frequency for the spells that the amplitudes dropped to less than unity was investigated for each station and the results are indicated in the last column of Table 8. The presented ratios vary from 1.5 in Shiraz to 3.8 in Lar, implying the significant role of the amplitude size on the frequency of heavy precipitation over the study area. According to the applied Mann–Whitney test, when MJO was in each of the phases 1, 2, 6, 7 and 8, compare to the spells that the amplitude size was lower than 1.0, the frequency of heavy precipitation was significantly improved for the spells that the amplitudes were bigger than unity (Table 8 last two rows). Inconsistent with these phases, the frequency of heavy precipitation was significantly greater when the MJO was in phase 5 and amplitudes were less than unity. The most important exception was found for Bushehr where the frequency of heavy precipitation was zero or 3 for the periods that the MJO was in phase 6 and amplitudes were greater or less than unity, respectively (Table 8).

Table 9 The dates of all heavy precipitation in Shiraz (5% threshold)

	January	February	March	April	November	December	Total
Phase 1	01.11.2002-1,45,*1;1.0* * 01.12.1996-1,40,*0;0.8* 01.10.1978-2,29,*2;0.7*		03.31.2009-*1*,31.5,*1;2.8* 03.25.1997-*1*,30.3,*1;3.5*			12.01.1986-*1*,99,*2;1.0* 12.02.1986-2,96,*1;0.9* 12.01.1997-1,39,*0;1.3* 12.22.1976-0,35,*0;0.6*	9-49.4**
Phase 2	01.14.1991-*1*,65,*1;0.4* 01.17.1996-0,44,*0;1.5* 01.18.1999-5,42.6,*0;1.7* 01.18.1988-2,38,*0;2.2*	02.06.1995-2,48,*2;0.4* 02.05.1995-1,35,*3;0.3*	03.26.2003-*1*,42,*1;1.2* 03.02.1999-3,32,*1;1.4* 03.11.2011-0,29.5,*2;1.1*		11.23.2011-*1*,29.3,*0;1.9*	12.06.2003-4,50,*0;1.5* 12.17.2006-1,47,*1;1.3* 12.19.1985-0,30,*1;0.2* 12.25.2004-0,30,*1;1.1*	14-40.2
Phase 3	01.14.2006-*3*,34.2,*0;1.3*	02.07.1995-*3*,33.4,*1;0.5*					2-33.8
Phase 4	01.22.1991-*4*,49,*2;1.5* 01.23.1991-5,38,*1;1.7* 01.24.1980-2,32,*0;1.0*	02.05.2003-*1*,41.2,*0;0.8*				12.21.1992-*1*,75,*1;0.4* 12.16.2004-3,61,*1;0.2*	6-49.4
Phase 5	01.17.2000-*1*,58,*0;0.4*			04.03.2002-*1*,30.1,*0;0.4*		12.15.2004-2,57,*2;0.6*	3-48.4
Phase 6	01.10.1979-0,46,*1;1.8* 01.02.1985-*1*,39,*2;0.8* 01.19.2005-2,37,*0;1.3* 01.02.1998-2,34,*0;1.2* 01.06.1977-*1*,33,*1;0.4* 01,28,1990-0,29,*1;2.4*	02.05.1999-*1*,30,*1;1.2*			11.29.2009-0,51.4,*0;1.4* 11.14.2005-2,45,*3;1.0* 11.13.2005-*1*,31,*4;0.8*	12.17.1980-*1*,57,*1;0.4* 12.13.2004-0,53.3,*4;0.5* 12.09.2004-1,44,*0;0.7* 12.04.1995-0,41.2,*2;1.1* 12.10.2000-1,31,*1;1.2*	15-40.1
Phase 7	01.09.2004-*3*,62,*5;2.8* 01.08.2004-2,56,*6;2.6* 01.03.1985-2,52,*1;0.5*	02.11.1980-*1*,35,*1;1.1* 02.08.1982-0,31,*1;0.7* 02.17.1988-*1*,31,*1;2.1*			11.19.1986-2,31,*1;1.4*	12.13.2001;*1*,49,*3;1.7* 12.05.1995;*1*,30.2,*1;1.0*	9-42.0
Phase 8	01.07.1988-*1*,57,*2;0.6* 01.10.2004-4,41,*4;2.8* 01.11.2004-5,39.1,*3;2.9* 01.09.1978-*1*,35,*3;0.6* *01.23.1979*-1,33,*1;2.2* 01.23.2005-1,31,*0;0.8* 01.11.1996-0,30.2,*1;0.5*	02.10.1976-0,41,*1;1.7* 02.21.1999-2,31,*1;2.1*	03.26.1977-0,39,*1;1.8* 03.04.1987-0,38,*0;1.9*			12.09.1992-*1*,58.1,*0;0.4* 12.26.1988-0,44,*1;0.9* 12.07.1991-0,40.2,*2;1.5* 12.08.2009-0,35.1,*1;0.7* 12.15.1989-3,30,*0;1.0*	16-38.9
Total	28–41.8***	10–35.7	7–34.6	1–38.0	5–37.5	23–49.2	74–42.1

The numbers of rainy days before and after heavy precipitation, the phase and amplitude of MJO during these dates, mean precipitation for each phase and each month are also presented

*The presented statistics in each line denote month, day, year, the number of precipitating days before the day of heavy precipitation, the amount of heavy precipitation, the number of rainy days after heavy precipitations and the MJO amplitude in the day of heavy precipitation, respectively. For example, in the first line heavy precipitation has occurred on 11 of January 2002. Precipitation had started a day before heavy precipitation. Total heavy precipitation was 45 mm and precipitation continued one day after the occurrence of heavy precipitation. Magnitude of the MJO amplitude was 1.0 for the day of heavy precipitation

**The presented statistics in the last column signify total frequency of heavy precipitation and its mean intensity during the indicated MJO phase. For instance, the frequency and mean precipitation during MJO phase 1 are 9 days and 40.2 mm/day, respectively

***The presented statistics in the last row signify total frequency of heavy precipitation and its mean intensity during the indicated month. For instance, the frequency and mean precipitation during January are 28 and 41.8 mm/day, respectively

5.3 Synoptic scale analysis

For result briefing, the illustrated Figs of this section are related to 74 days of heavy precipitation at Shiraz station (Tables 2, 9). In Table 9 the detail specification of these 74 days are presented. As indicated, most of the heavy precipitation has occurred during December–January period. After phase 8, the frequency of heavy precipitation at Shiraz is highest in phase 6. Although similar illustrations were also produced for other stations, due to general conformity with the presented discussion, some of these images are shown in the Appendix 1. Besides these 74 days of heavy precipitation and for consolidation of the results, similar Figs are also presented for a day before and a day after these days to consolidate the results. In other words, three sets of data comprising datasets for a day before heavy precipitation, day of the heavy precipitation and a day after precipitation were utilized to generate the presented composite images.
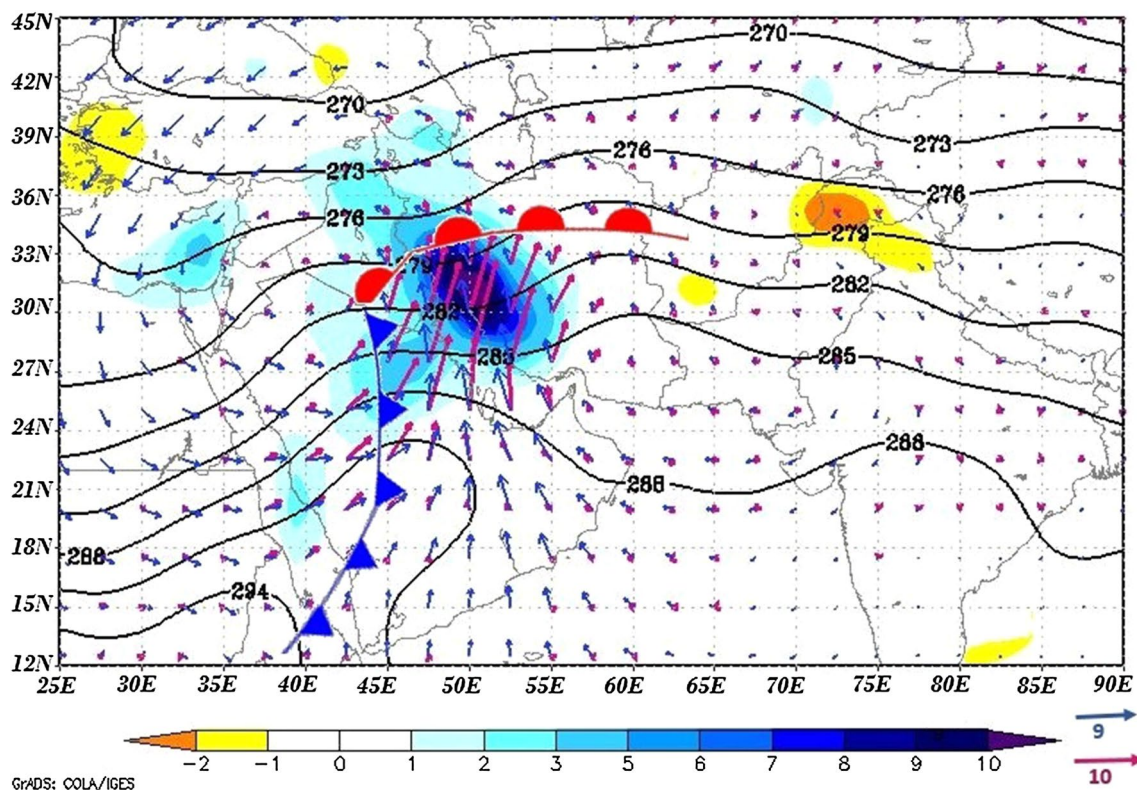
Fig. 2 The overlaid images of precipitation (mm/day), mean temperature (°K), the anomalies of vector wind (m/s) at the 850 hPa level and anomalies of vapor flux at 700 hPa level (g/kg m/s) at Shiraz station. All images were produced by compositing the relevant data of 74 days; all a day before heavy precipitation as indicated in. While *blue arrows* illustrate the main pattern of wind flow at 850 hPa level, *red arrows* depict the 700 hPa level vapor flux. Wind vectors are significantly greater than 9 m/s. The approximate position of the cold and warm fronts are shown by relevant meteorological symbols. The isotherms are separated by 3 °K intervals. Vapor flux is significantly greater than 10 g/kg*m/s. contains similar Figs but for the other stations

5.4 A day before heavy precipitation

Figure 2 illustrates the spatial distribution of the mean anomalies of precipitation at Shiraz station for 74 days; all a day before heavy precipitation. The precipitation image was then overlaid by corresponding images of some other atmospheric variables including wind vector and mean temperature at 850 hPa level as well as vapor flux at 700 hPa level. It is worthwhile to note that the arrows of wind vector and vapor flux were not distinguishable when these variables were selected from the same level. Our preliminary analysis proved a general conformity between this Fig and its corresponding Figs for the other stations as indicated in the Appendix 1. Due to such conformity, the presented discussion was found to be appropriate for demonstrating some synoptic-scale features of heavy precipitation in southwestern parts of Iran.

According to Fig. 2, for a day before heavy precipitation, a cyclonic circulation prevails over the western parts of the Middle East, mostly consisted of the areas in eastern parts of the Mediterranean Sea, north and west of Saudi Arabia, west of Iran and almost the entire parts of Iraq and Turkey.

The northerly wind in the western flank of this cyclonic system pushes the Mediterranean-based cold air masses toward the northern and western parts of Saudi Arabia. These air masses are generally cooler and dryer than the local air masses develop over the eastern and central parts of the Arabian Peninsula. As indicated in Fig. 2, in Egypt and northern parts of Saudi Arabia, isotherms are crossed by northerly wind vectors with a large angle that causes cold advection and air subsidence over these areas. On the other hand, the intersection of the southerly wind vectors with isotherms causes an intensified warm advection over the Persian Gulf and southwestern parts of Iran. An upward air motion and formation of warm front over these areas are the consequences of this warm advection.

Concurrent with the formation of this cyclonic airflow, an anti-cyclonic circulation prevails over the northwestern districts of India, northern parts of the Arabian Sea, the Persian Gulf and eastern edge of the Arabian Peninsula (Fig. 2). This clockwise circulation induces cold advection and air subsidence over northern parts of India and Pakistan as denoted by negative precipitation anomaly. The circulation, however, drags the warm-humid tropical air
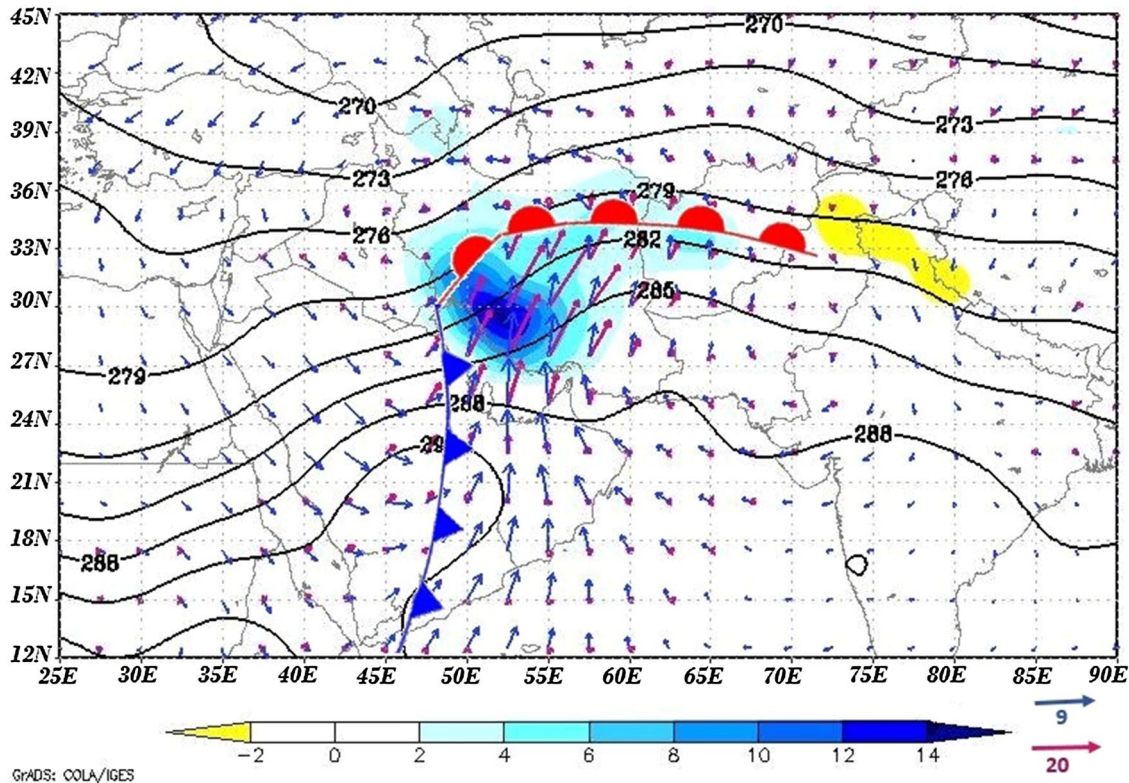
Fig. 3 Like Fig. 2 except for the day of heavy precipitation. The dates used for generating the presented images are exactly the dates of 74 days of heavy precipitation as denoted in. Wind vectors are significantly greater than 9 m/s. The delineated vapor flux is statistically greater than 20 g/kg*m/s

masses of the Arabian Sea into the eastern parts of the Arabian Peninsula, to be piled-up in the east of the mentioned cold air-mass. A cold front therefore develops in the interface of these two air-masses (Fig. 2). Some synoptic scale phenomena including deflection of wind direction from northwesterly in behind into southerly in ahead of the cold front, temperature gradient between these two sides of the front and precipitation event along and ahead of the front are the main specifications of this cold front (Fig. 2). As indicated, temperature difference between northwestern and southeastern parts of Saudi Arabia might exceed 6.0 °C for such dates. It is worthwhile to note that the southerly airflow ahead of the cold front re-moisturizes by the Persian Gulf; before encroaching Iran's territory. Northward propagation of these tropical air-masses triggers warm advection and formation of warm front in the southwest of Iran. Temperature anomaly was found positive over most parts of Saudi Arabia, Persian Gulf and Iran during a day before to a day after heavy precipitation (not shown).

According to Fig. 2, the heaviest precipitation generally occur over the Zagros highlands in the western parts of Iran and eastern side of Iraq to emphasize the simultaneous effects of topography and weather fronts in the production of highly intensified precipitation. For a day before heavy

precipitation, maximum anomalies of wind speed and precipitation were observed near the west coast of the Persian Gulf (Fig. 2). Alijani (2008) has also accentuated the role of these highlands for the intensification of frontal precipitation. The presented synoptic condition of heavy precipitation is somehow similar to the regional synoptic state during the cold months-dust storm in the Middle East as indicated by Notaro et al. (2013).

5.5 Heavy precipitation day

For the day of heavy precipitation, the mentioned atmospheric state including a cyclone, an anticyclone and the combination of cold and warm fronts moves further into the east (Fig. 3). Moreover, due to the intensification of wind speed, precipitation intensity also increases over most parts of southern Iran. Since land surface elevation in Saudi Arabia generally decreases eastward, the cold front, therefore, moves from relatively highland regions in the west to the substantially lower elevation areas in the central parts of this country. Therefore, the observed suppression in precipitation amount over Saudi Arabia could mostly be attributed to the topography rather than moisture-dependent parameters (compare Figs. 2, 3).
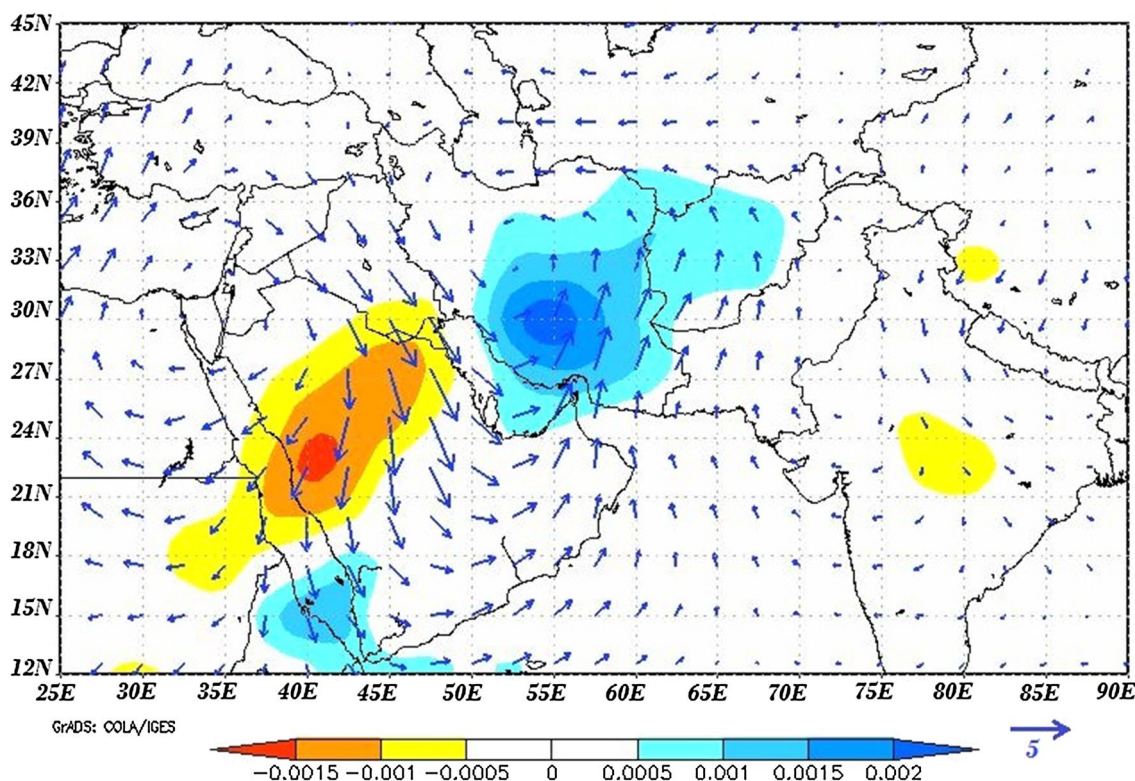
Fig. 4 The spatial distribution of the difference in specific humidity at 850 hPa level between the day of heavy precipitation and a day earlier (gr water/gr air). The specific humidity map is then imposed on the corresponding differential map of vector wind (m/s). Positive or negative values indicate increase or decrease in the humidity during the day of heavy precipitation as compared with a day earlier, respectively

Due to eastward propagation of the weather system, almost entire parts of the Persian Gulf and western corner of the Oman Sea re-moisturize the southerly airflows ahead of the cold front. At the 850 hPa pressure level, specific humidity in southern parts of Iran increases by about 2 gr/Kg in the day of heavy precipitation as compared to a day earlier (Fig. 4). In both Figs. 2 and 3 the magnitude of vapor flux in the northern parts of the Persian Gulf is considerably greater than corresponding values in the Arabian Peninsula. All these evidences emphasize the influential role of the Persian Gulf for re-moisturizing the weather system crossing this water body. The intensified passage of the moist southerly airflows over the areas with strong temperature gradient improves warm advection in the northern parts of the Persian Gulf. Therefore, precipitation increases over the areas extended from southwest of Iran to northwest of Afghanistan (Fig. 3). In contrast to Iran, specific humidity and precipitation substantially decreases in the northern and middle parts of Saudi Arabia.

5.6 A day after heavy precipitation

In its eastward propagation, the mentioned weather system moves toward northeastern parts of Iran during a day after heavy precipitation. While precipitation extends from southern districts of Iran to northern parts of Tajikistan, its core center is located over the mountainous areas of Afghanistan and Tajikistan (Fig 5). Temperature contrast between two sides of the cold front in Saudi Arabia is less than two earlier days and precipitation deficiency is evident over the Arabian Peninsula and southwestern parts of Iran (compare Figs. 3, 5).

It is worthwhile to note that the storm track from a day before to a day after heavy precipitation is not absolutely eastward as indicated by eastward propagation of the MJO signals over equatorial areas of the Indo-Pacific regions. Heavy precipitation generally tends to evolve over the areas comprising west of Iran, east of Iraq and northeast of Saudi Arabia. After crossing southwestern and central-southern parts of Iran, the weather system moves toward northeastern parts of the country and western corner of Afghanistan. The absence of significant highlands in the eastern parts of Iran and southwestern districts of Pakistan could be the external force that pushes the weather system northward.

Formation of warm front in the northeastern districts of Iran and particularly northern parts of Afghanistan and Tajikistan, enhances easterly circulation over some areas in the northern and eastern side of the front such as
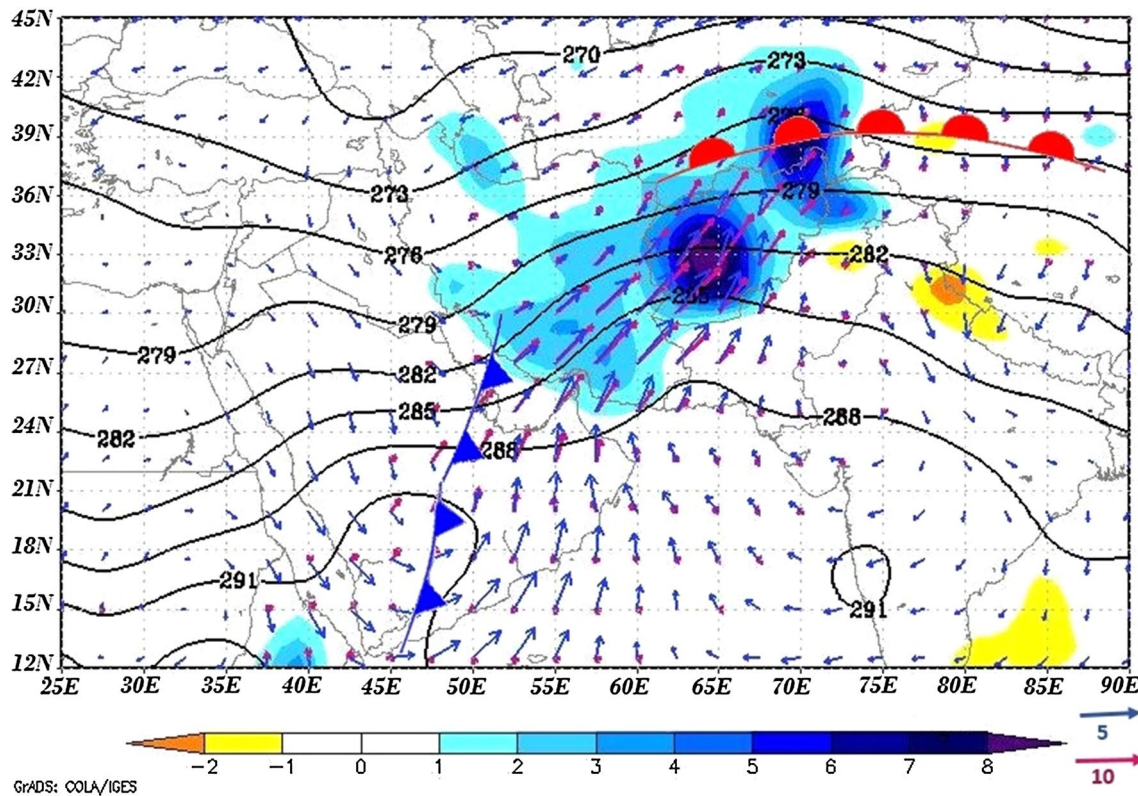
Fig. 5 Like Figs. 2 and 3 except for a day after heavy precipitation. The data of 74 days, all a day after the dates of heavy precipitation, were used for producing this Fig. Vector winds are significantly greater than 5 m/s. The presented *arrows* of vapor flux is statistically greater than 10 g/kg*m/s

southwestern parts of the Caspian Sea in Iran and southern districts of Azerbaijan (Fig. 5). Since the Caspian Sea moisturizes these easterlies, precipitation enhancement is evident over these regions during a day after heavy precipitation in southwestern parts of the country. The circulation, however, becomes a dry northerly airflow over most parts of Turkey to suppress precipitation over these areas.

6 Conclusions

The present study assessed some statistical and synoptically properties of the November–April heavy precipitation in the southwest of Iran for the period 1975–2011. The associations between this precipitation and the MJO were also investigated. Daily values of precipitation data in nine synoptic stations were analyzed for the studied period.

In spite of the fact that the frequency of considered precipitation accounted for 5% (or 10%) of total frequency of precipitating days, this precipitation constitutes about 25.7–35.8% (or 40.9–52.0%) of total annual precipitation. About 53% of the heavy precipitation events occurred during December–January period. This statistic is about 18, 15

and 9% for the months of March, February and November, respectively. A large portion of heavy precipitation was centered on phase 8 of the MJO. After this, heavy precipitation, respectively, centered on phases 2, 7, 1, 6, 5 and 4. By excluding phases 4 and particularly phase 5 of the MJO, the frequency and total precipitation significantly increased or decreased when the amplitude size was greater or less than unity.

Prevalence of a cold and cyclonic circulation over the eastern parts of the Mediterranean Sea and western parts of Saudi Arabia as well as blowing a vigorous warm anticyclonic flow over northern parts of the Arabian Sea was realized as the key elements for the occurrence of heavy precipitation over the studied areas. Development of a north–south oriented cold front that mostly locates in the middle parts of Saudi Arabia is the main consequence of these opposite airflows. In addition to precipitation production in Saudi Arabia, formation of this cold front pushes the accumulated warm-humid air-masses ahead of this cold front toward the Persian Gulf and southwestern parts of Iran.

Northward propagation of these tropical air-masses causes warm advection and formation of west-east oriented

warm fronts in various parts of Iran Afghanistan and Tajikistan. Formation of heavy precipitation was found to be associated to the formation of weather fronts over the highlands of these countries.
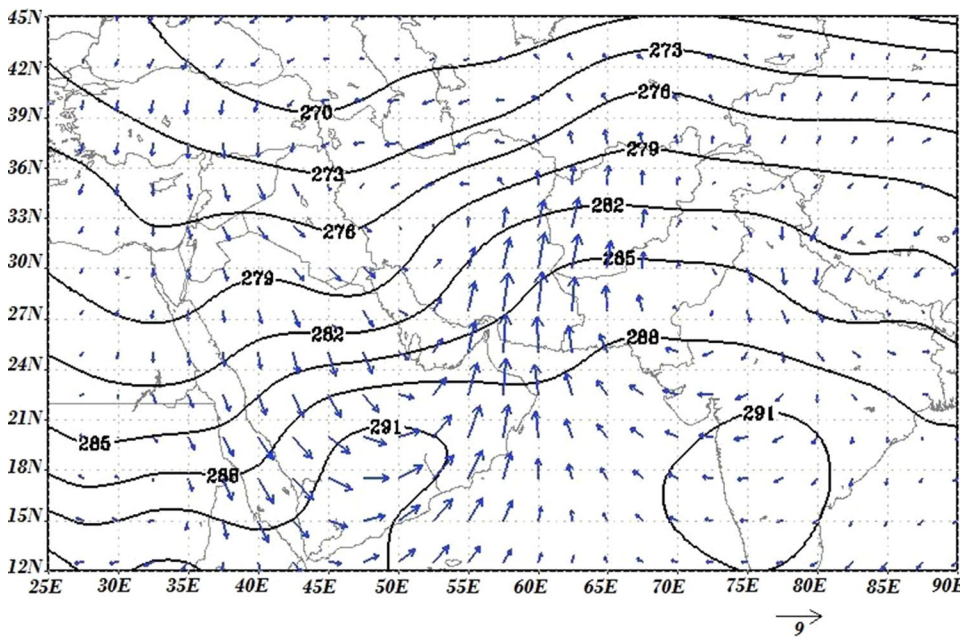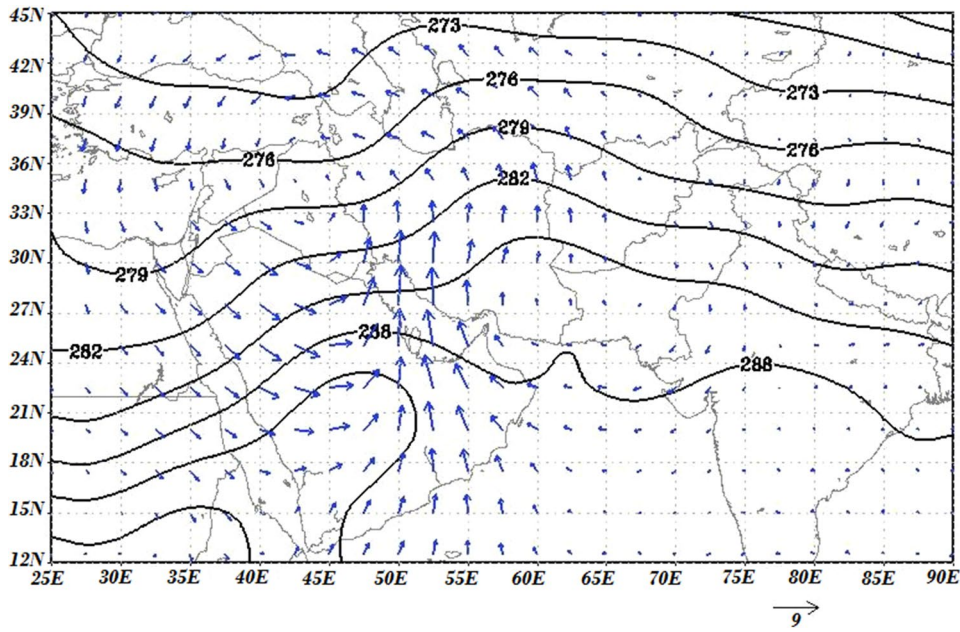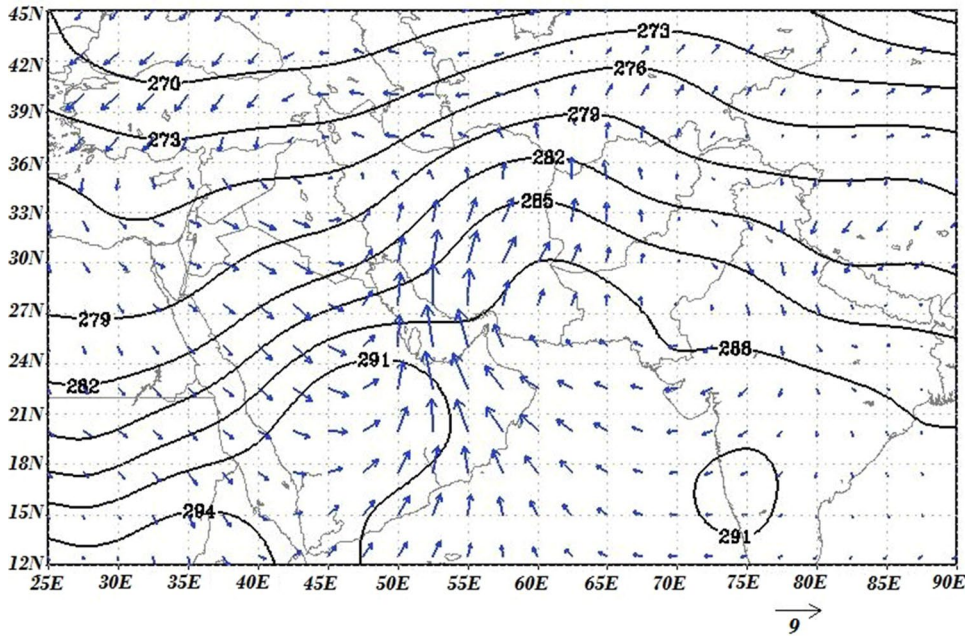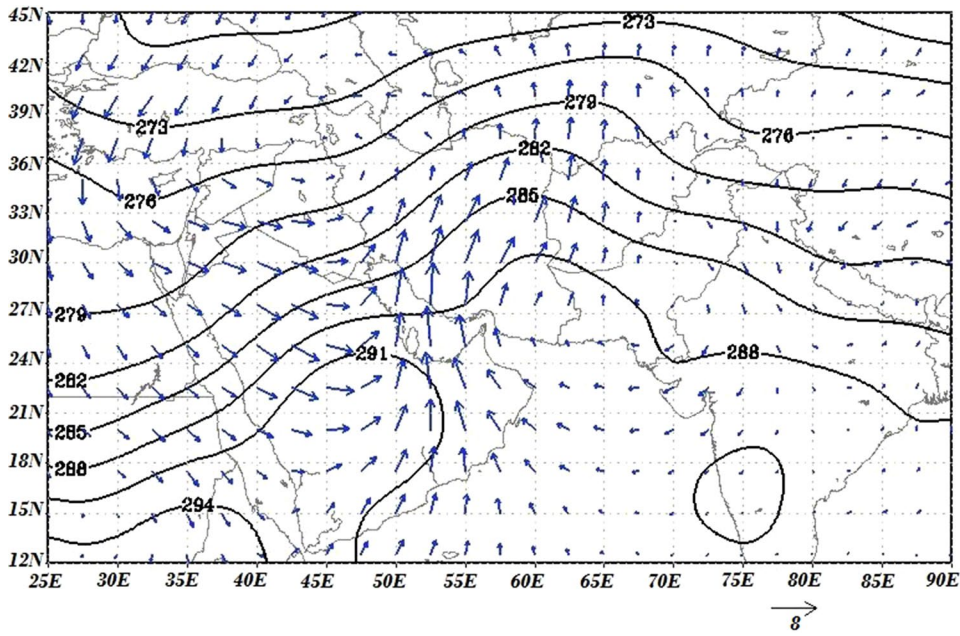
Appendix

The overlaid images of the mean temperature (oK) and the anomaly vector wind (m/s) at the 850 hPa level for the day of heavy precipitation at other stations except Shiraz station.
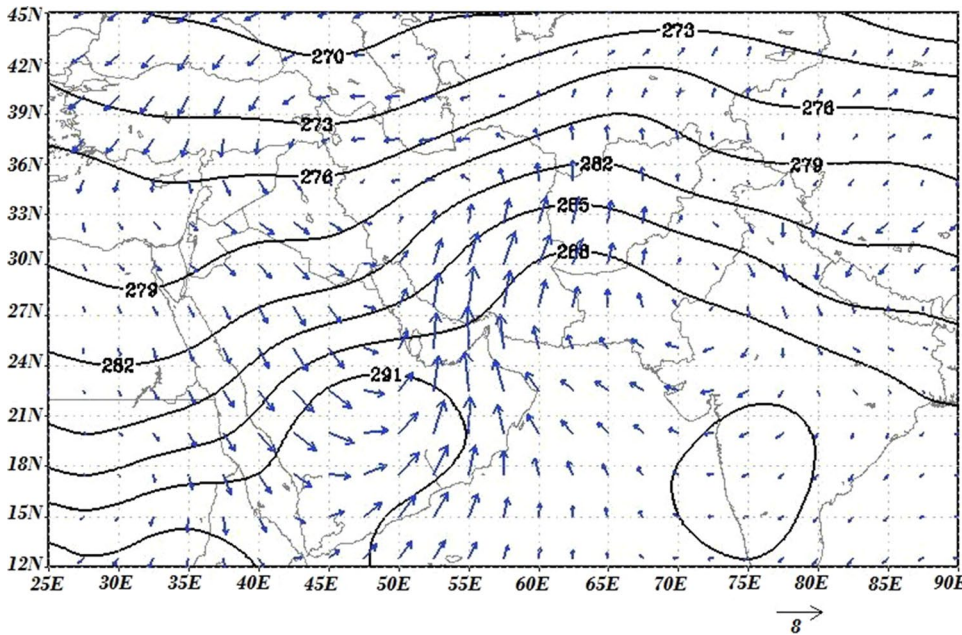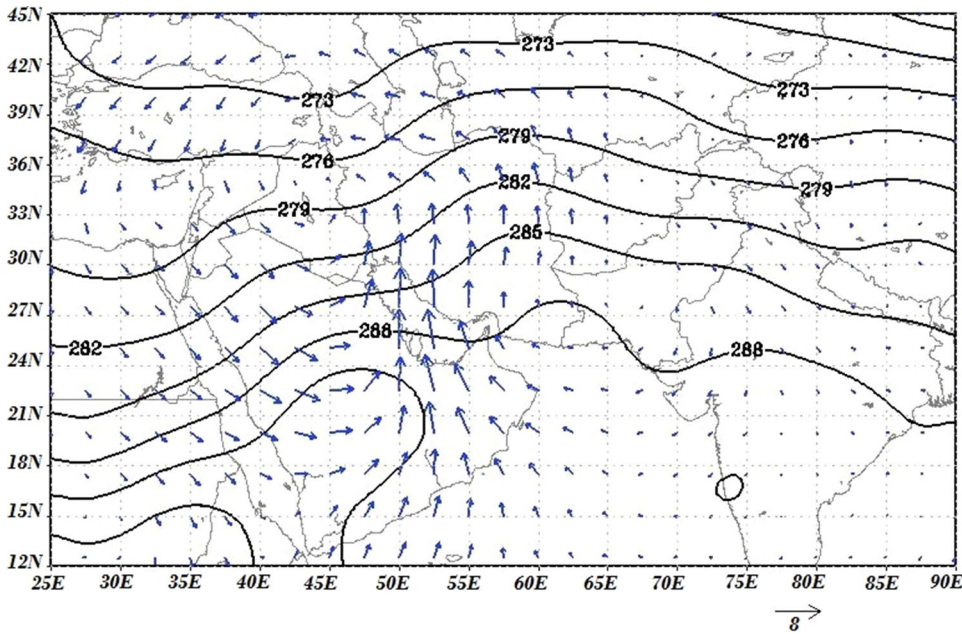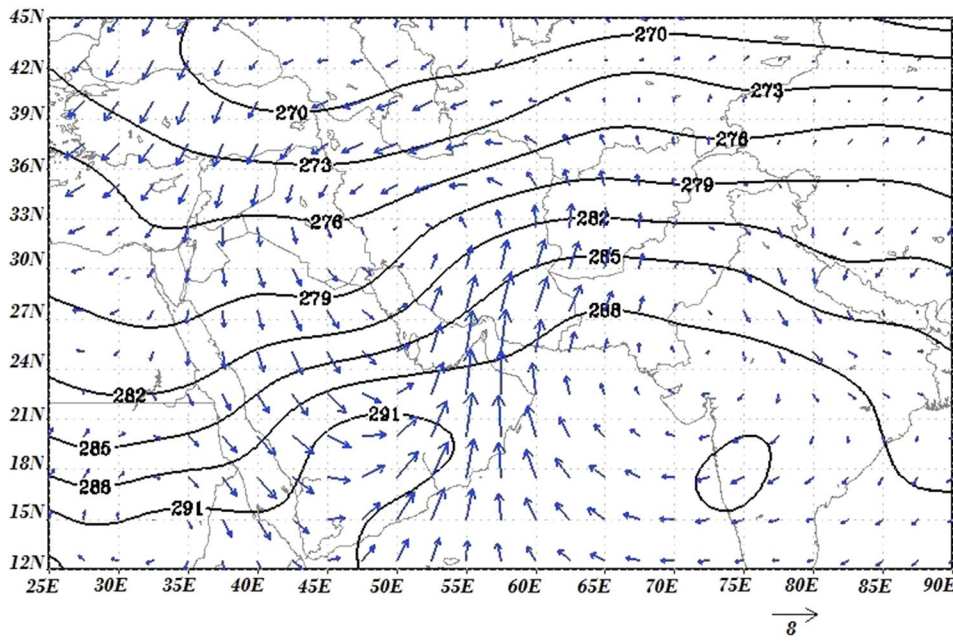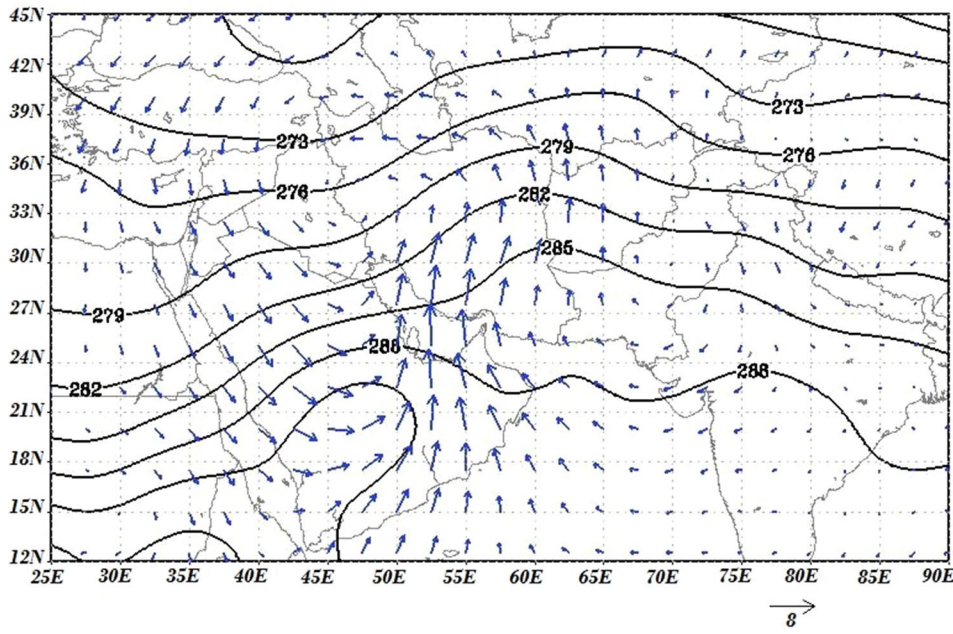
References

Adames AF, Wallace JM (2014) Three-dimensional structure and evolution of the MJO and Its relation to the mean flow. J Atmos Sci 71:2007–2026. doi:10.1175/JAS-D-13-0254.1

Adames AF, Wallace JM (2015) Three-dimensional structure and evolution of the moisture field in the MJO. J Atmos Sci 72:3733–3754. doi:10.1175/JAS-D-15-0003.1

Alijani B (2008) Effect of the Zagros Mountains on the spatial distribution of precipitation. J Mt Sci 5(3):218–231

Alijani B, O'brien J, Yarnal B (2007) Spatial analysis of precipitation intensity and concentration in Iran. Theor Appl Climatol 94 (1–2), 107–124

Alijani B, Khosravy M, Esmail-Nejad M (2010) A synoptic analysis of January 6, 2008 heavy precipitation in the southeast of Iran. J. Clim Res, fall 2010-winter 2011, 1 (3–4), 3–14

Barlow M, Cullen H, Lyon B (2002) Drought in Central and Southwest Asia: La Niña, the Warm Pool, and Indian Ocean Precipitation. J Clim 15:697–700. doi:10.1175/1520-0442(2002)015

Barlow M, Lyon B, Cullen H (2005) Modulation of daily precipitation over Southwest Asia by the Madden–Julian Oscillation. Mon Wea Rev 133: 3579–3594. doi:10.1175/MWR3026.1

Bond NA, Vecchi G (2003) The influence of the Madden-Julian Oscillation on precipitation in Oregon and Washington. J Wea Forecasting 18(4), 600–613

Carvalho LMV, Jones C, Liebmann B (2004) The South Atlantic convergence zone: Intensity, form, persistence and relationships with intraseasonal to interannual activity and extreme rainfall. J. Clim 17:88–108. doi:10.1175/1520-0442(2004)017<0088:TSACZI>2.0.CO;2

Donald A, Meinke H, Power B, Maia AHN, Wheeler MC, White N, Stone RC, Ribbe J (2006) Near-global impact of the Madden–Julian oscillation on rainfall. Geophy Res Lett 33, L09704 doi:10.1029/2005GL025155

Ferranti L, Palmer TN, Molteni F, Klinker K (1990) Tropical-extratropical interaction associated with the 30-60-day oscillation and its impact on medium and extended range prediction. J Atmos Sci 47:2177–2199. doi:10.1175/1520-0469(1990)047

Groisman PY, Knight RW, Easterling DR, Karl TR, Hegerl GC, Razuvaev VN (2004) Trends in Intense Precipitation in the Climate Record. J Clim 18:1326–1350. doi:10.1175/JCLI3339.1

Higgins RW, Shi W (2001) Intercomparison of the Principal Modes of Interannual and Intraseasonal Variability of the North American Monsoon System. J Clim 14:403–417. doi:10.1175/1520-0442(2001)

Hoell A, Funk C (2013) The ENSO-related west Pacific Sea surface temperature gradient. J Clim 26:9545–9562. doi:10.1175/JCLI-D-12-00344.1

Hoell A, Barlow M, Saini R (2012) The Leading Pattern of Intraseasonal and Interannual Indian Ocean Precipitation Variability and its Relationship with Asian Circulation during the Boreal Cold Season. J. Clim 25:7509–7526

Hoell A, Barlow M, Saini R (2013a) Intraseasonal and seasonal-to-interannual Indian Ocean convection and hemispheric teleconnections. J Clim 26(22):8850–8867. doi:10.1175/JCLI-D-12-00306.1

Hoell A, Funk C, Barlow M (2013b) The regional forcing of northern hemisphere drought during recent warm tropical west Pacific Ocean La Nina events. Clim Dyn, 1–23, doi:10.1007/s00382-013-1799-4

Hoell A, Funk C, Barlow M (2014) La Nina diversity and northwest Indian Ocean Rim teleconnections. Clim Dyn 43:2707–2724. doi:10.1007/s00382-014-2083-y

Hoell A, Shukla S, Barlow M, Cannon F, Kelley C, Funk C (2015) The forcing of monthly precipitation variability over Southwest Asia during the Boreal cold season. J Clim 28(18):7038–7056. doi:10.1175/JCLI-D-14-00757.1

Hung P-C, Yang T-H, Liaw H-J, Wu W-S (2014) The Yeast Nucleosome Atlas (YNA) database: an integrative gene mining platform for studying chromatin structure and its regulation in yeast. BMC Genom 15(Suppl 9):S5. doi:10.1186/1471-2164-15-S9-S5

Jones C (2000) Occurrence of extreme precipitation events in California and relationships with the Madden - Julian oscillation. J. Climate 13: 3576–3587. doi:10.1175/1520-0442(2000)013<3576:OOEPEI>2.0.CO;2

Kiladis GN, Coauthors (2014) A comparison of OLR and circulation-based indices for tracking the MJO. Mon Wea Rev 142:1697–1715

Krishnamurti R (1997) Convection induced by selective absorption of radiation: a laboratory model of conditional instability. Dynam. Atmos. Oceans 27:367–382. doi:10.1016/S0377-0265(97)00020-1

Lau KM, Chan PH (1986) Aspects of the 40–50 day oscillation during the northern summer as inferred from outgoing longwave radiation. Mon. Weather Rev., 114:1354–1367. doi:10.1175/1520-0493(1986)

Libmann B, Hartmann DL (1984) An observational study of tropical-midlatitude interaction on intraseasonal time scale during winter. J Atmos Sci 41:3333–3350. doi:10.1175/1520-0469(1984)041<3333:AOSOTI>2.0.CO;2

Liu P (2014) MJO structure associated with the higher-order CEOF modes. Climate Dyn 43:1939–1950

Liu P, Zhang Q, Zhang C, Zhu Y, Khairoutdinov M, Kim H-M, Schumacher C, Zhang M (2016) A revised real-time multivariate MJO index. Mon Wea Rev 144:627–642

Masoodian SA, Mohammadi B (2012) The analysis of frontogenesis frequency at time of super heavy rainfall in Iran. Geogr Res 27(104):1–24 (**In Persian**)

Masoudian M (2009) The topographical impact on effectiveness of flood protection measures, Ph.D. thesis, Kassel University, Kassel pp 133

Masoudian A, jafari shendi F (2015) The Relationship between Synoptic Systems Influencing Heavy Rainfall in the Northern Low Rainfall Region. Winter 18 (50):305–331

Mo KC (2000) The association between intraseasonal oscillations and tropical storms in the Atlantic basin. Mon Wea Rev 128:4097–4107. doi:10.1175/1520-0493(2000)

Nazemosadat MJ (2001) Winter rainfall in Iran: ENSO and aloft wind interactions. Iran J Sci Technol 25:611–624

Nazemosadat MJ, Cordery I (2000) On the relationships between ENSO and autumn rainfall in Iran. Int. J. Climatol 20:47–61. doi:10.1002/(SICI)1097-0088(2001)

Nazemosadat MJ, Ghaedamini H (2010) On the Relationships between the Madden–Julian Oscillation and Precipitation Variability in Southern Iran and the Arabian Peninsula: Atmospheric Circulation Analysis. J. Clim 23:887–904. doi:10.1175/2009JCLI2141.1

Nazemosadat MJ, Ghasemi AR (2004) Quantifying the ENSO-related shifts in the intensity and probability of drought and wet periods in Iran. J. Clim 17:4005–4018. doi:10.1175/1520-0442(2004)

Nazemosadat SMJ, Shahgholian K (2014) Formation of heavy precipitations in the southwestern part of Iran and its association with the Madden-Julian Oscillation. J Water Soil 28(5):1072–1083 (**In Persian**)

Nazemosadat MJ, Samani N, Barry DA, Molaii Niko M (2006) ENSO forcing on climate change in Iran: precipitation analyses. Iran J Sci Technol Trans B Eng 30(B4):47–61

Nogues-Paegle J, Byerle LA, Mo KC (2000) Intraseasonal modulation of South American summer precipitation. Mon Wea Rev 128, 837–850. doi:10.1175/1520-0493(2000)

Notaro M, Alkolibi F, Fadda E, Bakhrjy F (2013) Trajectory analysis of Saudi Arabian dust storms. J Geophys Res Atmos 118:6028–6043. doi:10.1002/jgrd.50346

Pourasghar F, Tozuka T, Ghaemi H, Oettli P, Jahanbakhsh S, Yamagata T (2015) Influences of the MJO on intraseasonal rainfall variability over southern Iran. Atmos Sci Lett 16:110–118

Ventrice MJ et al (2013) A modified multivariate Madden–Julian oscillation index using velocity potential. Mon Wea Rev 141:4197–4210

Wheeler MC, Hendon HH (2004) An all-season real-time multivariate MJO index: development of an index for monitoring and prediction. Bureau of Meteorology Research Centre, Melbourne, Australia. Mon Wea Rev 132:1917–1932 doi:10.1175/1520-0493(2004)

Zaitchik BF (2017) Madden–Julian Oscillation impacts on Tropical African precipitation. Atmos Res 184:88–102. doi:10.1016/j.atmosres.2016.10.002

Zhang C (2005) Madden–Julian oscillation. Rev Geophys 43:RG2003. doi:10.1029/2004RG000158